Syntheses, Structures, Magnetic Properties, and Density Functional Theory Magneto-Structural Correlations of Bis(µ-phenoxo) and Bis(µ-phenoxo)-µ-acetate/Bis(µ-phenoxo)-bis(µ-acetate) Dinuclear Fe(III)Ni(II) Compounds

Susanta Hazra,[†] Sagarika Bhattacharya,[†] Mukesh Kumar Singh,[‡] Luca Carrella,[§] Eva Rentschler,[§] Thomas Weyhermueller,[∥] Gopalan Rajaraman,*[,‡] and Sasankasekhar Mohanta*[,†]

[†]Department of Chemistry, University of Calcutta, 92 A. P. C. Road, Kolkata 700 009, India

[‡]Department of Chemistry, Indian Institute of Technology Bombay, Powai, Mumbai 400076, India

[§]Institut für Anorganische Chemie und Analytische Chemie, Johannes-Gutenberg Universität Mainz, Duesbergweg 10-14, D-55128 Mainz, Germany

[∥]Max-Planck-Institut für Chemische Energiekonversion, Stiftstr 34-36, 45470 Mülheim an der Ruhr, Germany

Ⓢ Supporting Information

$J = -3.14$ cm^{-1} $J = 7.36$ cm^{-1}
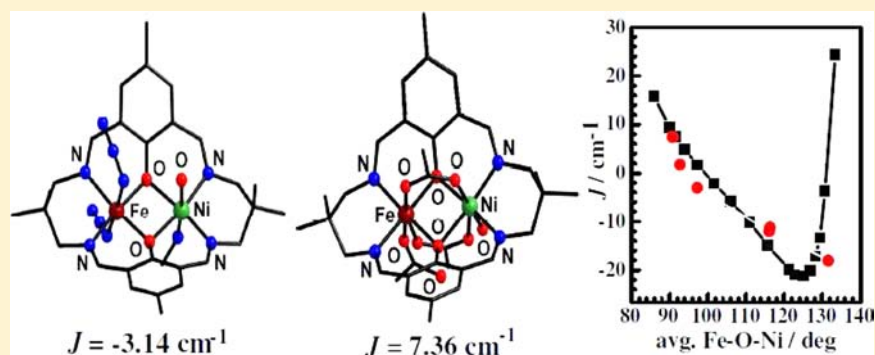
ABSTRACT: The bis(µ-phenoxo) Fe(III)Ni(II) compound $[Fe^{III}(N_3)_2LNi^{II}(H_2O)(CH_3CN)](ClO_4)$ (**1**) and the bis(µ-phenoxo)-µ-acetate/bis(µ-phenoxo)-bis(µ-acetate) Fe(III)Ni(II) compound $\{[Fe^{III}(OAc)LNi^{II}(H_2O)(\mu\text{-}OAc)]_{0.6}\cdot[Fe^{III}LNi^{II}(\mu\text{-}OAc)_2]_{0.4}\}(ClO_4)\cdot$ $1.1H_2O$ (**2**) have been synthesized from the Robson type tetraiminodiphenol macrocyclic ligand H_2L, which is the $[2 + 2]$ condensation product of 4-methyl-2,6-diformylphenol and 2,2′-dimethyl-1,3-diaminopropane. Single-crystal X-ray structures of both compounds have been determined. The cationic part of the dinuclear compound **2** is a cocrystal of the two species $[Fe^{III}(OAc)LNi^{II}(H_2O)(\mu\text{-}OAc)]^+$ (**2A**) and $[Fe^{III}LNi^{II}(\mu\text{-}OAc)_2]^+$ (**2B**) with weights of 60% of the former and 40% of the latter. While **2A** is a triply bridged bis(µ-phenoxo)-µ-acetate system, **2B** is a quadruply bridged bis(µ-phenoxo)-bis(µ-acetate) system. Variable-temperature (2−300 K) magnetic studies reveal antiferromagnetic interaction in **1** and ferromagnetic interaction in **2** with J values of −3.14 and 7.36 cm^{-1}, respectively ($H = -2JS_1 \cdot S_2$). Broken-symmetry density functional calculations of exchange interaction have been performed on complexes **1** and **2** and also on previously published related compounds, providing good numerical estimates of J values in comparison to experiments. The electronic origin of the difference in magnetic behavior of **1** and **2** has been well understood from MO analyses and computed overlap integrals of BS empty orbitals. The role of acetate and thus its complementarity/countercomplementarity effect on the magnetic properties of diphenoxo-bridged Fe(III)Ni(II) compounds have been determined on computing J values of model compounds by replacing bridging acetate and nonbridging acetate ligand(s) by water ligands in the model compounds derived from **2A,B**. The DFT calculations have also been extended to develop several magneto-structural correlations in these types of complexes, and the correlations focus on the role of Fe−O−Ni bridge angle, average Fe/Ni−O bridge distance, Fe−O−Ni−O dihedral angle, and out-of-plane shift of the phenoxo group.

■ INTRODUCTION

The phenomenon of magnetic exchange in discrete molecules was discovered/explained by Guha[1a] and Bleaney and Bowers[1b] in the early 1950s while studying the variable-temperature magnetic properties of diaqua-$\mu_{1,3}$-acetate dicopper(II). Over the decades, the magnetic properties of coordination compounds have received tremendous attention. Eventually, a number of experimental[2−7] and theoretical[2a,3d,f,4b−d,8−10] magneto-structural correlations were determined. Moreover, a number

of single-molecule magnets (SMMs)[11−16] have been developed with the aim of their possible application in molecular spintronics and quantum computing.[17] In fact, a renaissance has been continuing to develop 3d/4f/3d-4f-SMMs with greater blocking temperatures (T_B; the maximum to date is 8.3 K)[15c] and greater energy barriers (U_{eff}; the maximum to date is 556 cm^{-1})[15b] to magnetization reversal.

Developing magneto-structural correlations using only experimental means is a nontrivial task because this demands structurally similar or identical complexes with all but one governing parameter being identical. On the other hand, theoretical magneto-structural correlations can be more easily established because it is easily possible in most cases to construct model systems in which one parameter varies, keeping others constant.[3d,f,4b,d,8−10] Even when it is problematic to vary one parameter at a time for some heterobridged systems, theoretical correlations can be established defining new parameters, which are functions of two other parameters.[4c] Density functional theoretical (DFT) methods have been established as valuable tools in developing magneto-structural correlations and modeling the magnetic properties of the full structures of exchange-coupled systems to gain insight into the magnetic coupling mechanism and to analyze various contributions.[3d,f,4b−d,8−10,18]

The first and perhaps the most elegant magneto-structural correlation was determined experimentally in planar dihydroxo-bridged dicopper(II) compounds by Hatfield, Hodgson, and co-workers.[3a] The other types of homometallic systems for which experimental or theoretical magneto-structural correlations have been determined include alkoxo-bridged Cu^{II}_4 of cubane type,[3b] diphenoxo-bridged Cu^{II}_2,[3c,d,8a] roof-shaped dihydroxo-bridged Cu^{II}_2,[8b] monophenoxo-bridged Cu^{II}_2 having axial−equatorial bridging atoms,[3e] dihydroxo/dialkoxo-bridged Cu^{II}_2,[8c,d] linear Cu^{II}_3 having a diphenoxo bridge in a pair of metal ions,[3f] chloro-bridged Cu^{II}_2,[3g] dihalo-bridged Cu^{II}_2,[8e] bis($\mu_{1,1}$-azide) Cu^{II}_2,[8f,g] bis($\mu_{1,3}$-azide) Cu^{II}_2,[8g,h] diphenoxo-bridged Ni^{II}_2,[4a] bis($\mu_{1,1}$-azide) Ni^{II}_2,[8f,9] bis($\mu_{1,3}$-azide) Ni^{II}_2,[8h] bis($\mu_{oximate}$) Ni^{II}_2,[4b] heterobridged μ-phenoxo-$\mu_{1,1}$-azide Ni^{II}_2,[4c] $\mu_{1,3}$-azide Ni^{II}_4,[4d] oxo-bridged Fe^{III}_2,[5a,b] dialkoxo-bridged Fe^{III}_2,[5c,d] asymmetrically phenoxo-, alkoxo-, and hydroxo-bridged Fe^{III}_2,[5e] heterobridged Fe^{III}_2/Fe^{III}_3 having one oxo/hydroxo/alkoxo plus at least one carboxylate/sulfate/phosphate bridging moiety in a pair of metal ions,[5f] Fe^{III}_6 having a μ-hydroxo-bis(μ-carboxylate) or bis(μ-alkoxo)-μ-carboxylate in a pair of metal ions,[5g] bis($\mu_{1,1}$-azide) Mn^{II}_2,[8f] bis(μ-oxo) Mn^{IV}_2,[6a,b] and tris(μ-oxo)/tris(μ-hydroxo)/tris(μ-ethoxide)/tris(μ-chloride)/tris(μ-bromide)/tris(μ-iodide)/bis(μ-oxo)-μ-hydroxo/μ-oxo-bis(μ-hydroxo) $Mn^{IV}_2/Cr^{III}_2/V^{II}_2$.[6c] While several correlations have been determined in homometallic systems, they are few in heteronuclear systems; experimental correlations[7] in diphenoxo-bridged $Cu^{II}Gd^{III}$ and $Cu^{II}V^{IV}O$ compounds and theoretical correlations[10] in diphenoxo-bridged $Cu^{II}Gd^{III}$ and $Ni^{II}Gd^{III}$ systems are probably the only examples of straightforward magneto-structural correlations in heterometallic systems.

In the midst of the renaissance in the development of SMMs having greater T_B and U_{eff} values, the determination of magneto-structural correlations for scarcely investigated systems, such as FeNi compounds, deserves attention; only a few dinuclear $Fe^{III}Ni^{II}$ complexes have been reported to date and $Fe^{III}Ni^{II}$ complexes having one or more phenoxo/alkoxo/hydroxo bridges are scarce.[19] Therefore, we have been motivated to explore this area. Such compounds are also important from a biomimetic point of view, especially after the determination of the protein crystal structure of Fe−Ni hydrogenase, which has disclosed a

unique Fe−Ni heterometallic site.[20] Despite the fact that these dinuclear units are building blocks for several polynuclear FeNi complexes[21] and are important from the perspective of bio-mimetic chemistry, magneto-structural correlations for this pair have not been developed either experimentally or theoretically.

To isolate $Fe^{III}Ni^{II}$ compounds, we have chosen the mono-nuclear Fe^{III} compound $[Fe^{III}(H_2L)(H_2O)Cl](ClO_4)_2 \cdot 2H_2O$ as the precursor, where H_2L (Chart 1) is the symmetrical

Chart 1. Chemical Structure of H_2L
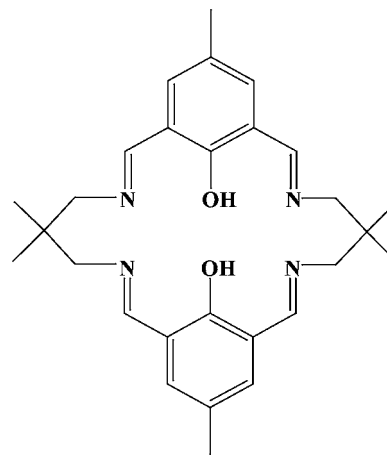
dinucleating Robson type[22] tetraiminodiphenolate macrocyclic ligand in which the dialdehyde counterpart is 4-methyl-2,6-diformylphenol and the diamine counterpart is 2,2′-dimethyl-1,3-diaminopropane.[14e] We anticipated that, on using secondary bridging ligands such as acetate and azide, the values of structural parameters involving the phenoxo bridges would be changed, which should affect the nature/magnitude of the magnetic exchange interaction. Again, the targeted systems having acetate/azide bridges should be interesting examples to explore complementarity/countercomplementarity effects in such complicated systems having so many combinations of magnetic orbitals. With all this in mind, we have isolated the bis(μ-phenoxo) $Fe^{III}Ni^{II}$ compound $[Fe^{III}(N_3)_2LNi^{II}(H_2O)(CH_3CN)](ClO_4)$ (**1**) and the cocrystalline bis(μ-phenoxo)-μ-acetate/bis(μ-phenoxo)-bis(μ-acetate) $Fe^{III}Ni^{II}$ compound $\{[Fe^{III}(OAc)LNi[Fe^{III}(OAc)LNi^{II}(H_2O)(\mu\text{-}OAc)]_{0.6} \cdot [Fe^{III}LNi^{II}(\mu\text{-}OAc)_2]_{0.4}\}(ClO_4) \cdot 1.1H_2O$ (**2**). Herein, we report the syntheses, crystal structures, and magnetic properties of **1** and **2** and density functional theoretical modeling of the magnetic properties of **1**, **2**, and related compounds along with DFT magneto-structural correlations.

■ EXPERIMENTAL SECTION

Materials and Physical Measurements. All of the reagents and solvents were purchased from commercial sources and used as received. The mononuclear iron(III) complex $[Fe^{III}(H_2L)(H_2O)(Cl)](ClO_4)_2 \cdot 2H_2O$ was prepared following the reported procedure.[14e] Elemental (C, H, and N) analyses were performed on a Perkin-Elmer 2400 II analyzer. IR spectra were recorded in the region 400−4000 cm^{-1} on a Bruker-Optics Alpha-T spectrophotometer with samples as KBr disks. Variable-temperature magnetic susceptibility measurements were carried out with a Quantum Design MPMS−XL7 SQUID magnetometer. Diamagnetic corrections were estimated from the Pascal constants. The temperature dependent magnetic contribution of the holder was experimentally determined and substracted from the measured susceptibility data.

Computational Details. There has been a great deal of interest in the evaluation of magnetic exchange couplings using the techniques of

quantum chemistry.[3d,f,4b−d,8−10,18] In dinuclear complexes the magnetic exchange interaction between Ni and Fe is described by the spin Hamiltonian

$$\hat{H} = -2J\hat{S}_{Fe}\hat{S}_{Ni} \qquad (1)$$

Here J is the isotropic exchange coupling constant and S_{Fe} and S_{Ni} are spins on iron(III) $(S = {}^5/_2)$ and nickel(II) $(S = 1)$ atoms, where a negative J value corresponds to an antiferromagnetic interaction. To compute the J values, the energies of the high-spin state $(S_T = {}^7/_2)$ and one low-spin state $(S_T = {}^3/_2)$ were calculated. The energy of the high-spin state can be computed straightforwardly using a single-determinant wave function such as DFT methods. Noodleman's broken-symmetry (BS) approach is used for the computation of the energy of the low-spin state of very large systems, which is derived from a spin-unrestricted reference wave function.[23] This BS approach consists of performing either unrestricted Hartree−Fock (UHF) or density functional theory (DFT) calculations for low-spin open-shell molecular systems in which the α and β densities are allowed to localize on different atomic centers, which are referred to as BS calculations. A detailed description of the computation of the magnetic exchange interaction can be found elsewhere.[18] Noodleman's BS approach and the widely used exchange-correlation functional B3LYP provide a good numerical estimate of the exchange coupling constant in comparison to experiment.[18] Accordingly, all calculations here we have used the B3LYP[24a] functional with the valence triple-ζ quality basis sets (TZV) of Ahlrichs and co-workers.[24b,c] All calculations were performed using the Gaussian 09 suite of programs.[25]

Syntheses of $[Fe^{III}(N_3)_2LNi^{II}(H_2O)(CH_3CN)](ClO_4)$ (1) and $\{[Fe^{III}(OAc)LNi^{II}(H_2O)(\mu\text{-}OAc)]_{0.6}\cdot[Fe^{III}LNi^{II}(\mu\text{-}OAc)_2]_{0.4}\}(ClO_4)\cdot 1.1H_2O$ (2). 2 was prepared by following a procedure similar to that described below for 1, except that solid NaOAc was used for 2 instead of solid NaN$_3$ for 1.

To a stirred acetonitrile/ethanol (1/1) solution (20 mL) of $[Fe^{III}(H_2L)(H_2O)(Cl)](ClO_4)_2\cdot 2H_2O$ (0.201 g, 0.25 mmol) under N$_2$ atmosphere were successively added solid NaN$_3$ (0.065 g, 1 mmol) and Ni(ClO$_4$)$_2\cdot$6H$_2$O (0.092 g, 0.25 mmol). After 4 h of stirring, the dark red solution was filtered to remove any suspended particles and the filtrate was kept at room temperature for slow evaporation. After 2 days, a dark violet crystalline compound containing diffraction-quality single crystals deposited. The compound was collected by filtration and washed with ethanol. Yield: 149 mg (73%). Anal. Calcd for C$_{30}$H$_{39}$N$_{11}$O$_7$ClFeNi: C, 44.17; H, 4.82; N, 18.89. Found: C, 44.21; H, 4.89; N, 18.85. IR (cm^{-1}, KBr): $\nu(H_2O)$, 3430 w; $\nu(N_3)$, 2048 vs; $\nu(C{=}N)$, 1630 vs; $\nu(ClO_4)$, 1089 vs, 620 w.

Data for 2 are as follows. Yield: 165 mg (80%). Anal. Calcd for C$_{32}$H$_{43.4}$N$_4$O$_{11.7}$ClFeNi: C, 46.78; H, 5.33; N, 6.82. Found: C, 46.45; H, 5.49; N, 6.64. IR (cm^{-1}, KBr): $\nu(H_2O)$, 3466 w; $\nu(C{=}N)$, 1640 s; $\nu_{as}(CO_2^-)$, 1571 m; $\nu_s(CO_2^-)$, 1430 m, 1400 m; $\nu(ClO_4)$, 1091 vs, 621 w.

Crystal Structure Determination of 1 and 2. The crystallographic data for 1 and 2 are summarized in Table 1. Diffraction data were collected on a Bruker-APEX II SMART CCD diffractometer at 296 K using graphite-monochromated Mo Kα radiation (λ = 0.71073 Å). For data processing and absorption correction the packages SAINT[26a] and SADABS[26b] were used. The structure was solved by direct and Fourier methods and refined by full-matrix least squares based on F^2 using the SHELXTL[26c] and SHELXL-97[26d] packages. The compound 2 is a cocrystal of two species, $[Fe^{III}(H_2O)LNi^{II}(OAc)(\mu\text{-}OAc)]^+$ (2A) and $[Fe^{III}LNi^{II}(\mu\text{-}OAc)_2]^+$ (2B), in amounts of about 60% and 40%, respectively (vide infra). Two hydrogen atoms of the coordinated water molecule in 2A and the hydrogen atoms of the water molecule of crystallization were not located and could not be inserted. On the other hand, the hydrogen atoms in 1 were located from a difference Fourier map. Other hydrogen atoms in 1 and 2 were inserted at calculated positions with isotropic thermal parameters and refined. Using anisotropic treatment for the non-hydrogen atoms and isotropic treatment for the hydrogen atoms, the final refinements converged at R1 values ($I > 2\sigma(I)$) of 0.0418 and 0.0453 for 1 and 2, respectively.

Table 1. Crystallographic Data for 1 and 2

	1	2
empirical formula	C$_{30}$H$_{39}$N$_{11}$O$_7$ClFeNi	C$_{32}$H$_{40}$N$_4$O$_{11.7}$ClFeNi
fw	815.73	817.89
cryst color	violet	violet
cryst syst	triclinic	monoclinic
space group	$P\bar{1}$	$P2/c$
a (Å)	9.2970(4)	11.7203(7)
b (Å)	10.3736(5)	16.0018(9)
c (Å)	18.8629(9)	22.9976(11)
α (deg)	104.5340(10)	90.00
β (deg)	94.7120(10)	117.610(3)
γ (deg)	101.1640(10)	90.00
V (Å^3)	1711.21(14)	3821.9(4)
Z	2	4
T (K)	293(2)	296(2)
2θ (deg)	2.26−50.98	2.54−51.64
μ (mm^{-1})	1.116	1.004
ρ_{calcd} (g cm^{-3})	1.583	1.421
$F(000)$	846	1698
abs cor	multiscan	multiscan
index range	−11 ≤ h ≤ 12	−12 ≤ h ≤ 14
	−12 ≤ k ≤ 12	−19 ≤ k ≤ 19
	−22 ≤ l ≤ 22	−28 ≤ l ≤ 28
no. of rflns collected	21105	47133
no. of indep rflns (R_{int})	6325 (0.0511)	7367 (0.0462)
R1^a/wR2^b ($I > 2\sigma(I)$)	0.0418/0.0976	0.0453/0.1168
R1^a/wR2^b (all F_o^2)	0.0655/0.1119	0.0743/0.1360

^{a}R1 = $[\sum\|\|F_o\| - \|F_c\|\|/\sum\|F_o\|]$. ^{b}wR2 = $[\sum w(F_o^2 - F_c^2)^2/\sum wF_o^4]^{1/2}$.

■ RESULTS AND DISCUSSION

Syntheses and Characterization. The two macrocyclic heterodinuclear Fe^{III}Ni^{II} complexes $[Fe^{III}(N_3)_2LNi^{II}(H_2O)(CH_3CN)](ClO_4)$ (1) and $\{[Fe^{III}(OAc)LNi^{II}(H_2O)(\mu\text{-}OAc)]_{0.6}\cdot[Fe^{III}LNi^{II}(\mu\text{-}OAc)_2]_{0.4}\}(ClO_4)\cdot 1.1H_2O$ (2) were readily obtained in high yield from the reaction mixture of $[Fe^{III}(H_2L)(H_2O)(Cl)](ClO_4)_2\cdot 2H_2O$, Ni(ClO$_4$)$_2\cdot$6H$_2$O, and sodium salt (NaN$_3$ for 1 and NaOAc for 2) of the appropriate secondary ligand in a 1:1:4 ratio.

The vibration due to the C=N bond appears at 1630 cm^{-1} for 1 and 1640 cm^{-1} for 2. The presence of perchlorates in 1 and 2 is evidenced by the appearance of the following infrared bands: a very strong band at 1089 cm^{-1} and a weak band at 620 cm^{-1} for 1, and a very strong band at 1091 cm^{-1} and a weak band at 621 cm^{-1} for 2. The water stretchings are observed at 3430 and 3466 cm^{-1}, respectively, for 1 and 2. A very strong signal at 2048 cm^{-1} in the spectrum of 1 indicates the presence of azide, whereas one $\nu_{as}(CO_2^-)$ vibration at 1571 cm^{-1} and two $\nu_s(CO_2^-)$ vibrations at 1430 and 1400 cm^{-1} in the spectrum of 2 suggest the presence of two types of acetate ligands.[19a] As will be seen below, the crystal structure of compound 2 contains both bridging and unidentate aceate ligands.

Description of the Structures of 1 and 2. Crystal structures of 1 and 2 are shown in Figures 1 and 2, respectively. The structures reveal that both are dinuclear Fe^{III}Ni^{II} compounds derived from the tetraiminodiphenolate macrocyclic ligand $[L]^{2-}$. In both compounds, one N$_2$O$_2$ compartment of $[L]^{2-}$ is occupied by a Fe^{III} ion, while the second N$_2$O$_2$ compartment is occupied by a Ni^{II} ion.

The metal centers in $[Fe^{III}(N_3)_2LNi^{II}(H_2O)(CH_3CN)](ClO_4)$ (1) are doubly bridged by the two phenoxo oxygen atoms. Both metal centers in 1 are hexacoordinated; the fifth and
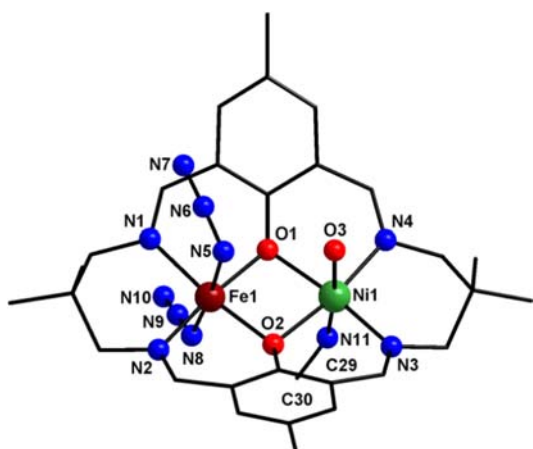
Figure 1. Crystal structure of $[Fe^{III}(N_3)_2LNi^{II}(H_2O)(CH_3CN)](ClO_4)$ (**1**). The perchlorate anion and all hydrogen atoms are omitted for clarity.

sixth coordination positions of the iron(III) center are occupied by two nitrogen atoms of two terminal azide ligands, while the fifth and sixth coordination positions of the nickel(II) center are provided by a water oxygen atom and an acetonitrile nitrogen atom.

The cationic part of the dinuclear compound $\{[Fe^{III}(OAc)\text{-}LNi^{II}(H_2O)(\mu\text{-}OAc)]_{0.6}\cdot[Fe^{III}LNi^{II}(\mu\text{-}OAc)_2]_{0.4}\}(ClO_4)\cdot 1.1H_2O$ (**2**) is a cocrystal of the two species $[Fe^{III}(H_2O)\text{-}LNi^{II}(OAc)(\mu\text{-}OAc)]^+$ (**2A**) and $[Fe^{III}LNi^{II}(\mu\text{-}OAc)_2]^+$ (**2B**) with weights of 60% of the former and 40% of the latter. While **2A** is a triply bridged bis(μ-phenoxo)-μ-acetate system, **2B** is a quadruply bridged bis(μ-phenoxo)-bis(μ-acetate) system. The iron(III) and nickel(II) centers in both **2A** and **2B** are hexacoordinated. The two species **2A** and **2B** have the common two N_2O_2 compartments (one for Fe^{III} and the second for Ni^{II}) and the common bis(μ-phenoxo)-μ-acetate bridging core, but they differ in terms of the sixth coordination positions; the sixth coordination positions of iron(III) and nickel(II) in **2A** are occupied by a monodentate acetate ligand (through O6) and a water oxygen atom (O4), respectively, and thus the bridging moiety is bis(μ-phenoxo)-μ-acetate, while the sixth coordination positions of the two metal centers in **2B** are occupied by a

bridging acetate ligand (through O4′ to Ni^{II} and through O6′ to Fe^{III}) and thus the bridging core is bis(μ-phenoxo)-bis(μ-acetate).

The hexacoordinated coordination environments for iron(III) and nickel(II) in **1** and **2** are distorted octahedral, in which the basal positions are occupied by the imine nitrogen and phenoxo oxygen atoms.

Selected bond lengths and bond angles of **1** and **2** are given in Tables 2 and 3, respectively. The two iron−phenoxo, iron−imine, nickel−phenoxo, or nickel−imine bond distances in both compounds are very close. Again, in both compounds, the two

Table 2. Selected Bond Lengths (Å) and Bond Angles (deg) in the Coordination Environments of the Metal Centers in 1

Bond Lengths			
Ni1−O1	2.052(2)	Fe1−O1	1.993(2)
Ni1−O2	2.062(2)	Fe1−O2	1.988(2)
Ni1−N3	1.994(3)	Fe1−N1	2.064(3)
Ni1−N4	1.998(3)	Fe1−N2	2.050(3)
Ni1−O3	2.125(3)	Fe1−N5	2.149(3)
Ni1−N11	2.075(3)	Fe1−N8	2.027(3)
		Fe1···Ni1	3.038

Bond Angles			
O1−Ni1−N3	170.45(10)	O1−Fe1−N2	172.87(11)
O2−Ni1−N4	171.18(11)	O2−Fe1−N1	171.89(10)
O3−Ni1−N11	174.51(11)	N5−Fe1−N8	174.97(12)
O3−Ni1−O1	86.41(9)	N5−Fe1−O1	87.31(10)
O3−Ni1−O2	87.61(9)	N5−Fe1−O2	87.47(10)
O3−Ni1−N3	89.71(11)	N5−Fe1−N1	85.50(11)
O3−Ni1−N4	88.58(10)	N5−Fe1−N2	89.91(11)
N11−Ni1−O1	88.16(11)	N8−Fe1−O1	93.23(11)
N11−Ni1−O2	90.80(10)	N8−Fe1−O2	97.55(11)
N11−Ni1−N3	95.54(12)	N8−Fe1−N1	89.49(12)
N11−Ni1−N4	92.25(11)	N8−Fe1−N2	90.11(12)
O1−Ni1−O2	81.03(9)	O1−Fe1−O2	84.35(9)
O1−Ni1−N4	90.79(11)	O1−Fe1−N1	91.27(10)
O2−Ni1−N3	90.09(10)	O2−Fe1−N2	88.97(10)
N3−Ni1−N4	97.84(12)	N1−Fe1−N2	95.06(11)
		Fe1−O1−Ni1	97.39(10)
		Fe1−O2−Ni1	97.22(10)

(a) **2A**   (b) **2B**
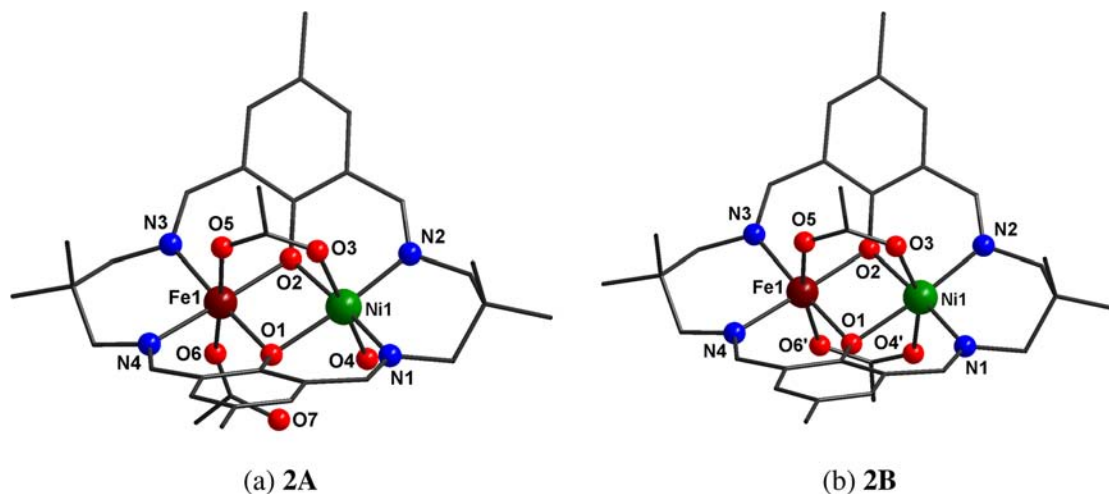
Figure 2. Crystal structure of $\{[Fe^{III}(OAc)LNi^{II}(H_2O)(\mu\text{-}OAc)]_{0.6}\cdot[Fe^{III}LNi^{II}(\mu\text{-}OAc)_2]_{0.4}\}(ClO_4)\cdot 1.1H_2O$ (**2**; 60% **2A** + 40% **2B**): (a) $[Fe^{III}(OAc)LNi^{II}(H_2O)(\mu\text{-}OAc)]^+$ (**2A**); (b) $[Fe^{III}LNi^{II}(\mu\text{-}OAc)_2]^+$ (**2B**). The perchlorate anion, water of crystallization, the minor component of the disordered methyl carbon atom of the common bridging acetate, and all of the hydrogen atoms are omitted for clarity.

Table 3. Selected Bond Lengths (Å) and Bond Angles (deg) in the Coordination Environments of the Metal Centers in 2 (2A + 2B)

Bond Lengths			
Ni1−O1	2.054(2)	Fe1−O1	2.003(2)
Ni1−O2	2.057(2)	Fe1−O2	2.005(2)
Ni1−N1	2.028(3)	Fe1−N3	2.050(3)
Ni1−N2	2.006(3)	Fe1−N4	2.054(3)
Ni1−O3	2.055(2)	Fe1−O5	2.049(2)
Ni1−O4/O4′	2.053(6)[a]/2.196(9)[b]	Fe1−O6/O6′	2.002(8)[c]/2.028(13)[d]
		Fe1···Ni1	2.8923(7)

Bond Angles			
O1−Ni1−N2	175.21(11)	O1−Fe1−N3	176.72(11)
O2−Ni1−N1	175.24(11)	O2−Fe1−N4	176.04(11)
O3−Ni1−O4/O4′	176.28(18)[a]/158.6(2)[b]	O5−Fe1−O6/O6′	177.29(15)[c]/165.3(2)[d]
O1−Ni1−N1	88.23(11)	O1−Fe1−N4	88.61(11)
O1−Ni1−O2	87.47(9)	O1−Fe1−O2	90.34(9)
O1−Ni1−O3	85.48(9)	O1−Fe1−O5	85.97(9)
O1−Ni1−O4/O4′	94.46(17)[a]/77.0(2)[b]	O1−Fe1−O6/O6′	96.60(18)[c]/81.7(3)[d]
O2−Ni1−N2	88.81(11)	O2−Fe1−N3	87.74(10)
O2−Ni1−O3	86.04(9)	O2−Fe1−O5	86.34(9)
O2−Ni1−O4/O4′	90.25(17)[a]/81.2(3)[b]	O2−Fe1−O6/O6′	94.5(2)[c]/85.7(4)[d]
O3−Ni1−N1	91.59(12)	O5−Fe1−N3	91.25(11)
O3−Ni1−N2	91.26(12)	O5−Fe1−N4	89.78(11)
N1−Ni1−N2	95.37(13)	N3−Fe1−N4	93.13(12)
N1−Ni1−O4/O4′	92.12(19)[a]/99.8(3)[b]	N3−Fe1−O6/O6′	86.21(19)[c]/100.8(3)[d]
N2−Ni1−O4/O4′	88.57(18)[a]/105.4(3)[b]	N4−Fe1−O6/O6′	89.4(2)[c]/97.9(4)[d]
		Fe1−O1−Ni1	90.96(9)
		Fe1−O2−Ni1	90.81(9)

[a]For O4 (in **2A**). [b]For O4′ (in **2B**). [c]For O6 (in **2A**). [d]For O6′ (in **2B**).

iron−phenoxo bond distances (average 1.990 Å in **1** and 2.003 Å in **2**) are shorter than the two nickel−phenoxo bond distances (average 2.057 Å in **1** and 2.055 Å in **2**). In contrast, the iron−imine bond distances (average 2.057 Å in **1** and 2.052 Å in **2**) are longer than the nickel−imine bond distances (average 1.996 Å in **1** and 2.017 Å in **2**). Of the two axial iron−azide bond distances in **1**, that (ca. 2.027 Å) involving N8 is in the range (ca. 1.990−2.057 Å) of the basal bond distances, while that (ca. 2.149 Å) involving N5 is significantly longer, while both the two axial bond distances (ca. 2.075 and 2.125 Å) involving nickel in **1** are longer than the basal bond distances (1.994−2.062 Å).

As already mentioned, one bridging acetate is common in **2A,B**. For this common acetate bridge, the iron−acetate (ca. 2.049 Å) and nickel−acetate (ca. 2.055 Å) bond distances are very close. However, for the second bridging acetate in **2B**, the nickel−acetate bond distance (ca. 2.191 Å) is significantly longer than the iron−acetate bond length (ca. 2.029 Å).

The iron(III)···nickel(II) separation in **1** (3.038 Å) is longer than that in **2** (2.892 Å). The phenoxo bridge angles in **1** (Fe1−O1−Ni1 = 97.39° and Fe1−O2−Ni1 = 97.22°) are almost identical, as are the two phenoxo bridge angles in **2** (Fe1−O1−Ni1 = 90.96° and Fe1−O2−Ni1 = 90.81°). Clearly, the phenoxo bridge angles in **2** are smaller than those in **1**. The dihedral angles between the two $N(imine)_2O(phenoxo)_2$ basal planes in **1** and **2** are 7.24 and 11.1°, respectively, indicating that the bridging moieties in both compounds are slightly twisted.

There exist a few intra-/intermolecular hydrogen bonding interactions in both **1** and **2**, some of which interlink the individual dinuclear units to generate a one-dimensional topology in **2** and a two-dimensional topology in **1** (see the Supporting Information for a description, demonstration (Figures S1 and S2), and geometries of the hydrogen bonds (Table S1)).

Magnetic Properties. dc magnetic susceptibility data were collected for crushed crystalline samples of **1** and **2** at an applied magnetic field of 1 T in the 2−300 K temperature range. The data of **1** and **2** are shown in Figures 3 and 4, respectively, as $\chi_M T$ versus T plots.
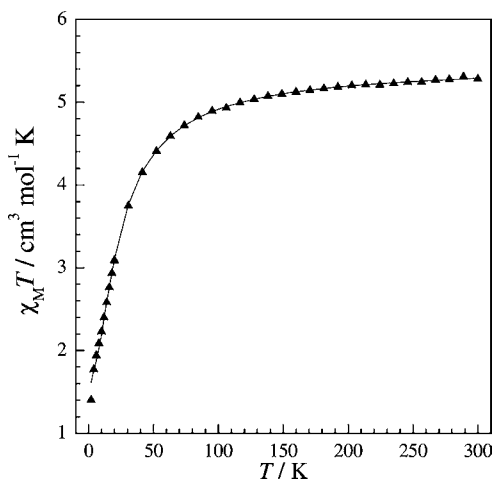

Figure 3. Fitting of the $\chi_M T$ versus T plot of $[Fe^{III}(N_3)_2LNi^{II}(H_2O)-(CH_3CN)](ClO_4)$ (**1**) between 2 and 300 K. The experimental data are shown as black triangles, and the black line corresponds to the theoretical values (see text).

For **1**, the $\chi_M T$ value at 300 K, 5.28 cm^3 mol^{-1} K, is only slightly less than the expected value of 5.38 cm^3 mol^{-1} K for one high-spin Fe^{III} ion ($S = {}^5/_2$) and one high-spin Ni^{II} ion ($S = 1$) with $g = 2.0$. As the temperature decreases from 300 to 60 K, the $\chi_M T$
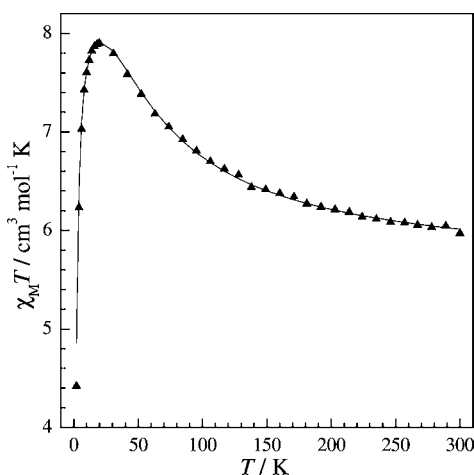
Figure 4. Fitting of the $\chi_M T$ versus T plot of {[Fe^{III}(OAc)LNi^{II}(H$_2$O)-(μ-OAc)]$_{0.6}$·[Fe^{III}LNi^{II}(μ- OAc)$_2$]$_{0.4}$}(ClO$_4$)·1.1H$_2$O between 2 and 300 K. The experimental data are shown as black triangles, and the black line corresponds to the theoretical values (see text).

product decreases slowly to 4.60 cm^3 mol^{-1} K. On further lowering of the temperature, $\chi_M T$ decreases rapidly to 1.40 cm^3 mol^{-1} K at 2 K. Clearly, the $\chi_M T$ versus T profile indicates that the Fe^{III} and Ni^{II} centers in **1** are antiferromagnetically coupled.

In the case of **2**, the $\chi_M T$ value at 300 K, 5.97 cm^3 mol^{-1} K, is greater than the expected value of 5.38 cm^3 mol^{-1} K for one high-spin Fe^{III} ion ($S = \frac{5}{2}$) and one high-spin Ni^{II} ion ($S = 1$) with $g = 2.0$. As the temperature decreases from 300 K, the $\chi_M T$ product increases steadily to reach a maximum of 7.90 cm^3 mol^{-1} K at 20 K. On further cooling to 2 K, the $\chi_M T$ product decreases rapidly to 4.42 cm^3 mol^{-1} K. The profile in this case clearly indicates ferromagnetic coupling between the two metal centers.

The susceptibility data were fitted using juIX software,[27] in which $H = -2JS_1 \cdot S_2$ is taken as the model Hamiltonian for dinuclear systems. To consider the intermolecular interaction which may propagate through the hydrogen-bonding interactions in **1** and **2**, the Weiss constant Θ was taken into consideration in the simulation process. It is also worth mentioning that an average J value was considered for **2A,B** and this approximation is highly logical because most of the structural parameters that may govern magnetic properties in **2A,B** are identical and the countercomplementarity effect of acetate is rather small (see below). The fittings converged with $J = -3.14$ cm^{-1}, $g_{Fe} = 2.0$, and

$g_{Ni} = 2.094$ for **1** and $J = 7.36$ cm^{-1}, $g_{Fe} = 2.0$, $g_{Ni} = 2.2$, and $\Theta = -0.75$ K for **2**. It is relevant to mention that, as compound **2** is a cocrystal of 60% of **2A** and 40% of **2B**, the J value of 7.36 cm^{-1} is actually the sum of the 60% of the J value of **2A** and 40% of the J value of **2B**. In fact, the DFT-computed J value of **2** has been calculated in this way (vide infra, footnotes of Table 4).

Comparison of Structures and Magnetic Properties of 1 and 2 with those of Related Compounds. Previously the Fe^{III}Ni^{II} compound [Fe^{III}(H$_2$O)L^{X}Ni^{II}(OAc)(μ-OAc)](ClO$_4$)·2H$_2$O (**3**), derived from a tetraaminodiphenol macrocyclic ligand, H$_2$L^X (the saturated analogue of a tetraiminodiphenolate macrocycle obtained on 2:2 condensation of 2,6-diformyl-4-methylphenol and 1,3-diaminopropane), has been reported.[19a] The metal centers in **3**, as in **2**, are bridged by a bis(μ-phenoxo)-μ-acetate moiety. Regarding dinuclear Fe^{III}Ni^{II} compounds having a phenoxo/hydroxo/alkoxo bridging moiety, only four other examples are known.[19b−d,28] Three of these are the heter-obridged μ-phenoxo-bis(μ-carboxylate) compounds [Fe^{III}Ni^{II}-(BPMP)(μ-OPr)$_2$](BPh$_4$)$_2$ (**4**),[19b] [Fe^{III}Ni^{II}(BPBPMP)(μ-OAc)$_2$](ClO$_4$) (**5**),[28] and [Fe^{III}Ni^{II}(IPCPMP)(μ-OAc)$_2$-(CH$_3$OH)] (PF$_6$) (**6**),[19c] where BPMP, BPBPMP, and IPCPMP are the anions of 2,6-bis[[(bis(2-pyridylmethyl)amino]methyl]-4-methylphenol, 2-bis[{(2-pyridylmethyl)-aminomethyl}-6-{(2-hydroxybenzyl)(2-pyridylmethyl)}aminomethyl]-4-methylphe-nol, and 2-(N-isopropyl-N-((2-pyridyl)methyl)aminomethyl)-6-(N-(carboxylmethyl)-N-((2-pyridyl)methyl)aminomethyl)-4-methylphenol, respectively. On the other hand, the remaining compound is the heterobridged μ-alkoxo-μ-diphenylphosphate system [Fe^{III}Ni^{II}(HPTB){μ-O$_2$P(OPh)$_2$}{O$_2$P(OPh)$_2$}-(CH$_3$OH)](ClO$_4$)$_2$·2H$_2$O (**7**),[19d] where HPTB is the anion of N,N,N′,N′-tetrakis(2-benzimidazolylmethyl)-2-hydroxy-1,3-dia-minopropane.

As compounds **1−3** contain a diphenoxo bridging moiety, parameters such as Fe−O−Ni bridge angles, Fe−O/Ni−O bridge distances, Fe−O−Ni−O dihedral angles, and out-of-plane shifts of the phenoxo group should be considered as the possible governing factors to determine the nature and extent of magnetic exchange interactions. For **2** and **3**, due to the presence of an additional carboxylate bridge, the effect of orbital complemen-tarity or orbital countercomplementarity should also have a role on the magnetic properties. On the other hand, as compounds **4−7** contain a monophenoxo (for **4−6**) or monoalkoxo (for **7**) bridging moiety, Fe−O−Ni bridge angles and Fe−O/Ni−O bridge distances should be considered as the possible governing

Table 4. Experimental and DFT-Computed J Values along with Some Relevant Structural Parameters of 1, 2, and Previously Published Related Fe^{III}Ni^{II} Compounds

complex[a]		J_{DFT} (cm^{-1})	J_{exp} (cm^{-1})	av Fe−O−Ni (deg)	av M−O (Å)	Fe−O−Ni−O (deg)	τ (Å)[b]	ref
[Fe^{III}(N$_3$)$_2$LNi(H$_2$O)(CH$_3$CN)]$^+$ (**1**)	bis(μ-phenoxo)	−4.5	−3.14	97.33	2.0262	0.9	30.95	this work
{[Fe^{III}(OAc)LNi^{II}(H$_2$O)(μ-OAc)]$_{0.6}$·[Fe^{III}LNi^{II}(μ-OAc)$_2$]$_{0.4}$}$^+$ (**2**)	bis(μ-phenoxo)-μ-acetate; bis(μ-phenoxo)-bis(μ-acetate)	7.23[c] (7.86 for **2A** 6.28 for **2B**)	7.36	90.88	2.0295	4.88	39.05	this work
[Fe^{III}(H$_2$O)L^{X}Ni^{II}(OAc)(μ-OAc)]$^+$ (**3**)[d]	bis(μ-phenoxo)-μ-acetate		1.7	92.8	2.0825	NA[e]	NA[d]	19a
[Fe^{III}Ni^{II}(BPMP)(OPr)$_2$]$^{2+}$ (**4**)	μ-phenoxo-bis(μ-propionate)	−13.2	−12	116.2	1.989			19b
[Fe^{III}Ni^{II}(BPBPMP)(OAc)$_2$]$^+$ (**5**)	μ-phenoxo-bis(μ-acetate)	−6.86	NA	118.66	2.026			25
[Fe^{III}Ni^{II}(IPCPMP)(μ-OAc)$_2$(CH$_3$OH)] (PF$_6$) (**6**)	μ-phenoxo-bis(μ-acetate)	−8.27	−11.2	116.43	2.014			19c
[FeNi(HPTB){μ-O$_2$P(OPh)$_2$}{O$_2$P(OPh)$_2$}(CH$_3$OH)]$^{2+}$ (**7**)	μ-alkoxo-μ-diphenylphosphate	−15.6	−18.1	131.7	2.0185			19d

[a]The formula of only the cationic part is given; see text for the composition of L^1, BPMP, BPBPMP, and HPTB. [b]Out-of-plane shift of the phenoxo group. [c]Calculated from 60% of [Fe^{III}(H$_2$O)LNi^{II}(OAc)(μ-OAc)]$^+$ (**2A**; J_{DFT} = 7.86 cm^{-1}) and 40% of [Fe^{III}LNi^{II}(μ-OAc)$_2$]$^+$ (**2B**; J_{DFT} = 6.28 cm^{-1}). [d]J_{DFT} value has not been computed because structural data are not available (see text). [e]Not available.

factors to determine the nature and extent of magnetic exchange interactions. For these compounds 4−7, orbital complementarity/countercomplementarity of carboxylates/phosphate bridging moieties should also have roles in the magnetic behavior. Of compounds 3−7, the magnetic properties of all but 5 were investigated. The observed J values (of 1−4, 6, and 7) along with the structural parameters (of 1−7), which may influence the magnetic properties, have been given in Table 4. While compounds 2 and 3 exhibits ferromagnetic interactions with J values of 7.36 and 1.7 cm^{-1}, respectively, the metal centers in compounds 1, 4, 6, and 7 are antiferromagnetically coupled with J values of −3.05, −12, −11.2, and −18.1 cm^{-1}, respectively.

It has been established in different types of systems that the nature and magnitude of magnetic exchange interactions are very much dependent on the bridge angle.[2,3a−g,4a,5a−d,6a,8a,c−g,9] The general trend in oxo/hydroxo/alkoxo-bridged systems is that interaction becomes less antiferromagnetic as the bridge angle becomes smaller; below a particular angle, the crossover angle, the interaction becomes ferromagnetic.[2,3a−f,4a,5a−d,8a,c,d] The crossover angle as determined from magneto-structural correlations in some systems are 97.5° in planar dihydroxo-bridged Cu$^{II}_2$,[3a] 95.7° in alkoxo-bridged Cu$^{II}_4$,[3b] 89° in diphenoxo-bridged Cu$^{II}_2$,[3d] 97° in diphenoxo-bridged Ni$^{II}_2$,[4a] and 91.2° in dialkoxo-bridged Fe$^{III}_2$.[5c] Even in monophenoxo-bridged Cu$^{II}_2$ compounds having an axial−equatorial mode of the bridging atom, a general trend of angle dependence of the exchange interaction has been observed.[3e] In that case, the ferromagnetic interaction becomes smaller as the bridge angle increases from 126° and the interaction becomes nil when the bridge angle is 142°. The general trend of angle dependence of exchange interaction has also been observed also in oxo-bridged Fe$^{III}_2$,[5a,b] dioxo-bridged Mn$^{IV}_2$,[6a] and Fe$^{III}_6$ compounds having μ-hydroxo-bis(μ-carboxylate)/bis(μ-alkoxo)-μ-carboxylate bridges.[5g] Now, the average phenoxo-bridge angle and the J value in the Fe^{III}Ni^{II} compounds 1−3, all having a common diphenoxo bridging moiety, are 97.33° and −3.14 cm^{-1} for 1, 92.8° and 1.7 cm^{-1} for 3, and 90.88° and 7.36 cm^{-1} for 2, revealing that the well-known general trend of bridge angle dependence of exchange integral is maintained here also. Similarly, although the Fe^{III}Ni^{II} compounds 4, 6, and 7 have a monophenoxo bridging moiety, stronger antiferromagnetic (J ranges between −11.2 and −18.1 cm^{-1}) interaction in these compounds in comparison to that in 1−3 is probably related to the greater values of Fe−O−Ni bridge angle (range 116.2−131.7°) in the former three compounds.

Although the exchange interactions can be qualitatively rationalized in terms of the bridge angle, it is relevant to know the roles of different parameters in a quantitative way as well as to understand the electronic origin of exchange interaction. To compute the theoretical J values, to understand the role of the aforementioned different factors on magnetic properties, and to determine magneto-structural correlations, DFT calculations have been carried out for compounds 1, 2, and 4−7 and for model systems. The DFT calculation on 3 could not be done because required structural data are not available in the CSD.[29] It may also be noted that the refinement of the structure of 3 was hampered ($R = 0.123$) due to the rather inferior quality of diffraction data and severe disordering of the perchlorate anions.[19a] The theoretical studies are described in the following section.

Theoretical Studies. DFT calculations have been performed on the full structures of complexes 1, 2, and 4−7, including the counteranion wherever applicable, and the results are summarized in Table 4. Of these six compounds, observed J values for compounds

1, 2, 4, 6, and 7 are available and it is interesting to note that an excellent agreement with the experimental J values has been obtained in all five of these systems. In this series of complexes, one can classify three types of interactions: (i) moderately weak antiferromagnetic interactions (complexes 1 and 5), (ii) moderately strong antiferromagnetic interactions (complexes 4, 6, and 7), (iii) moderately weak ferromagnetic interactions (complex 2). DFT calculations have nicely reproduced this trend; in fact, in all cases an excellent agreement with experimental J values has been detected.

Additionally, our aim has been to understand the electronic origin of the difference in the magnetic coupling (antiferro−ferro) observed between complexes 1 and 2 and then to develop extensive magneto-structural correlations for this class of compounds. To understand the difference in the magnetic coupling strength, we have performed MO analysis and computed overlap integrals using BS empty orbitals which are in many instances shown to be useful in performing qualitative analysis of the coupling mechanism.[30] As there is no crystallographic symmetry in these complexes, there are in principle 10 interactions possible between the magnetic orbitals of Ni(II) and Fe(III). We have computed the overlap integral for complex 1, and the following interactions are found to be significant: $d_{z^2}|p|d_{yz}$, $d_{z^2}|p|d_{z^2}$, $d_{z^2}|p|d_{x^2-y^2}$, $d_{x^2-y^2}|p|d_{z^2}$, and $d_{x^2-y^2}|p|d_{x^2-y^2}$ (see Figure 5). Since
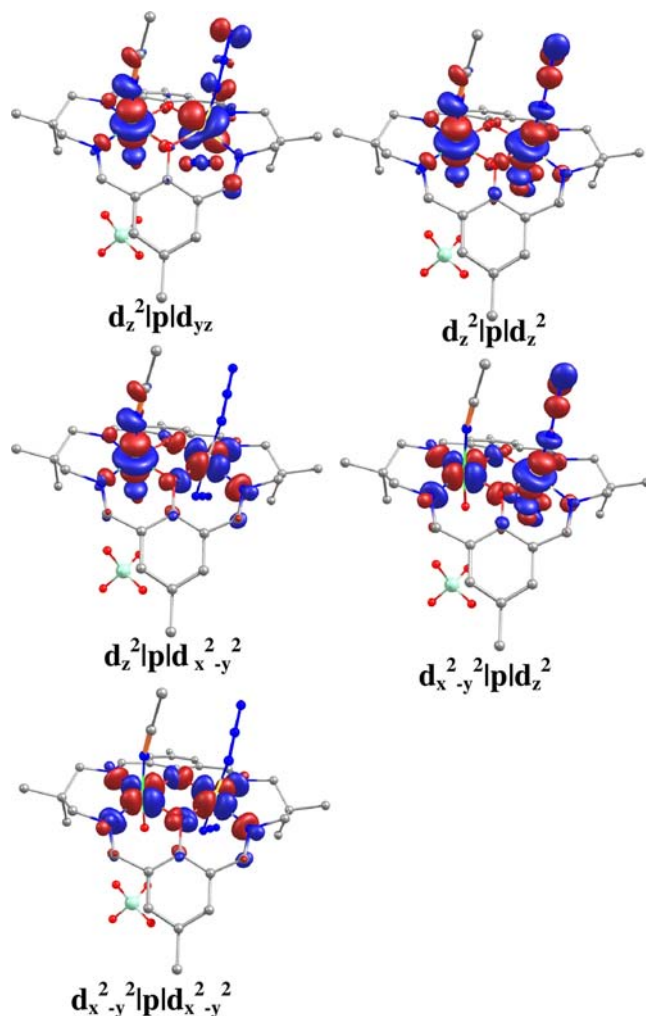

Figure 5. Pair of BS empty magnetic orbitals (for complex 1) where a significant overlap integral has been computed. The α set on Ni^{II} and β set of orbitals on Fe^{III} are plotted simultaneously for clarification.

the overlap integral is directly proportional to the antiferromagnetic part of the coupling constant, these five dominant interactions lead to antiferromagnetic coupling in complex **1**. It is important to note here that, out of these five interactions, the interactions between the axial orbitals are expected to dominate over the others ($d_{z^2}-d_{z^2}$ and/or $d_{x^2-y^2}-d_{x^2-y^2}$). For the species **2A** in complex **2**, significant interactions (see Figure 6) are
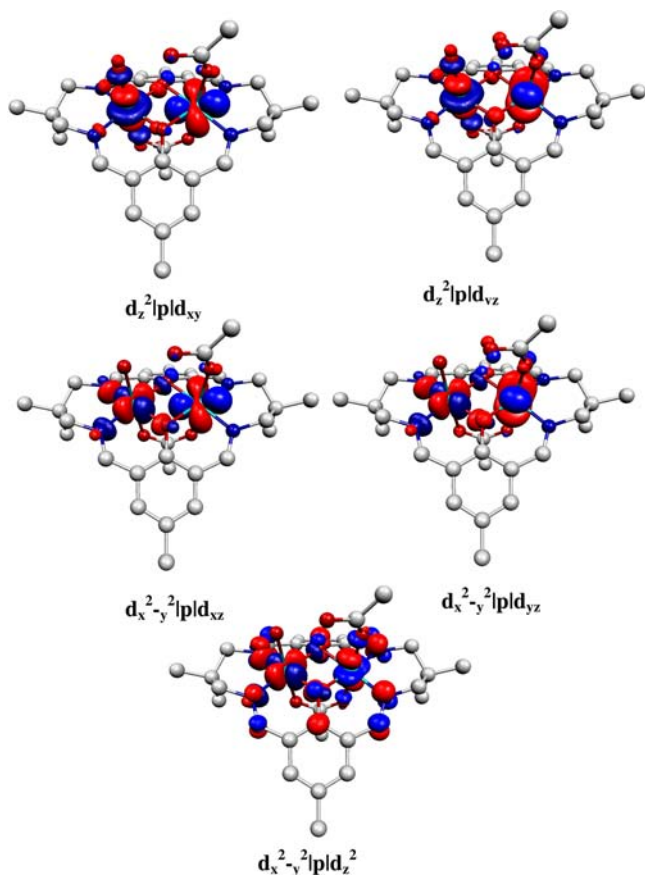

Figure 6. Pair of BS empty magnetic orbitals (for complex **2A**) where a significant overlap integral has been computed. The α set on Ni^{II} and β set of orbitals on Fe^{III} are plotted simultaneously for clarification.

$d_{z^2}|p|d_{xy}$, $d_{z^2}|p|d_{yz}$, $d_{x^2-y^2}|p|d_{xz}$, $d_{x^2-y^2}|p|d_{yz}$, and $d_{x^2-y^2}|p|d_{z^2}$. Although this complex also possesses five significant interactions, the $d_{z^2}|p|d_{z^2}$ and $d_{x^2-y^2}|p|d_{x^2-y^2}$ interactions are found to be less significant and this is likely due to the relatively acute Fe−O−Ni angle observed in complex **2** (90.87° in **2** versus 97.31° in **1**). In addition, it is important to note here that, due to the shorter Fe−Ni distance in complex **2**, some new interactions which are less significant in **1** are noticed ($d_{z^2}|p|d_{xy}$ and $d_{x^2-y^2}|p|d_{xy}$). For the species **2B** in complex **2**, seven strong interactions (see Figure 7) are observed: $d_{z^2}|p|d_{xz}$, $d_{z^2}|p|d_{yz}$, $d_{z^2}|p|d_{z^2}$, $d_{z^2}|p|d_{x^2-y^2}$, $d_{x^2-y^2}|p|d_{xy}$, $d_{x^2-y^2}|p|d_{z^2}$, and $d_{x^2-y^2}|p|d_{x^2-y^2}$. Clearly, the number of interactions is more in **2B** than in **2A**. Out of the seven interactions in **2B**, $d_{x^2-y^2}|p|d_{x^2-y^2}$ is the strongest. Therefore, because of the higher number of strong interactions, **2B** is expected to have a lower positive *J* value than **2A**. It is worth mentioning that the higher number of interactions in **2B** in comparison to those in **2A** arises because of the monodentate (to Fe^{III}) acetate ligand in **2A** versus bridging acetate ligand in **2B**, which is the only structural difference between **2A** and **2B**.

Apart from the differences in the bond angles, additional carboxylates (one for **2A** and two for **2B**) present in **2** may
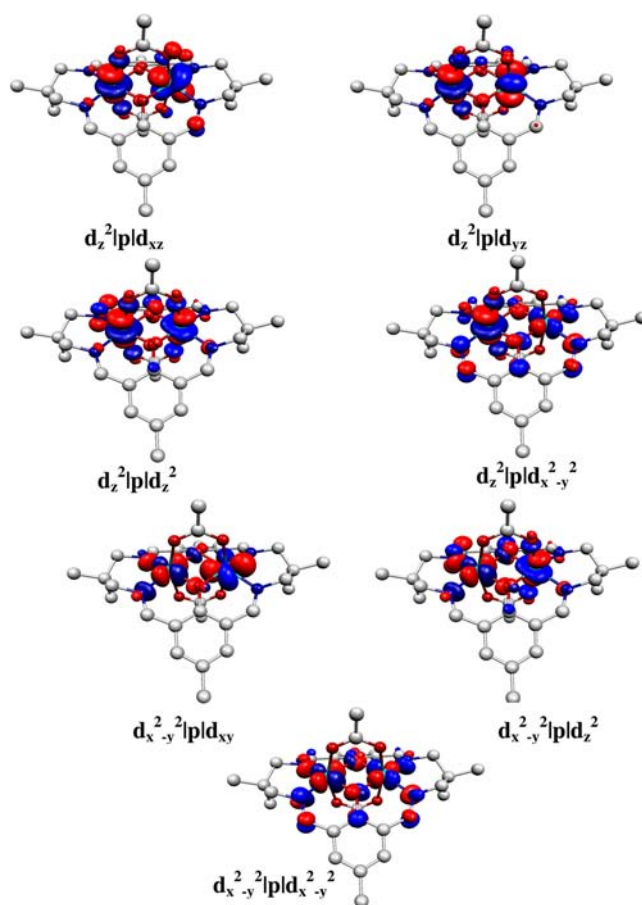

Figure 7. Pair of BS empty magnetic orbitals (for complex **2B**) where a significant overlap integral has been computed. The α set on Ni^{II} and β set of orbitals on Fe^{III} are plotted simultaneously for clarification.

bring forth complementarity/countercomplementarity effects. To understand the complementarity/countercomplementarity effects of the acetate group, calculations have been performed on model complexes constructed from **2A,B**. In the first model, $[Fe^{III}(H_2O)_2LNi^{II}(\mu\text{-OAc})]^{2+}$, the terminal acetate in **2A** coordinated to Fe(III) ion is modeled as a water molecule, and here a decrease in the ferromagnetic *J* value from 7.9 cm^{-1} (J_{DFT} value of **2A**) to a value of 5.7 cm^{-1} has been observed. When the bridging acetate is also modeled as water molecules, the *J* value further decreases to 5.3 cm^{-1}. A detailed discussion about complementarity/countercomplementarity effects are given in ESI (See Scheme S1 and the relevant discussion in the ESI). Clearly, the terminal acetate has a greater effect on the *J* value in comparison to the bridging acetate and the electronic reasons for this behavior are routed back to the interaction with the magnetic orbitals where the terminal acetate is found to have a stronger antibonding interactions with Fe (see Figure 6) in comparison to the bridging acetate. At this point, it is worth mentioning that the electronic effect of the coligands on exchange interactions is known.[31]

Both acetates in **2B** are also modeled as water ligands sequentially where the computed *J* values are 5.74 and 5.30 cm^{-1}, respectively, in comparison with 6.28 cm^{-1} (J_{DFT} value of **2B**). This suggests a countercomplementarity effect: i.e., the presence of terminal acetate enhances the strength of ferromagnetic *J* in this complex.

The spin density plots of complexes **1** and **2** (**2A** and **2B**) are shown in Figure 8. In both cases the spin density of Fe^{III} is found to be ∼4.2 while that on Ni^{II} is ∼1.7, revealing that spin delocalization is operative in both complexes. In both complexes,
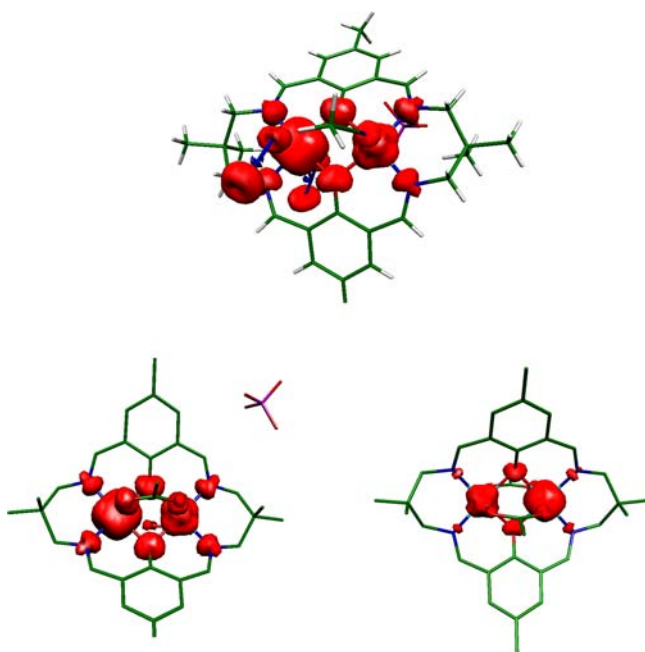
Figure 8. Computed spin density plots for complexes **1** (top) and **2** (bottom; **2A** left, **2B** right).

Figure 9. Magneto-structural correlation of average Fe−O−Ni bond angle of the model complex **1A** (as shown in Figure S4 in the Supporting Information) along with the experimental data points (shown by red dots; see Table 4).

the two μ-phenoxo oxygen atoms have different magnitudes of spin densities (for high-spin state: 0.12 and 0.14 in **1**, 0.16 and 0.15 in **2A**, and 0.15 and 0.15 in **2B**) and this is likely due to the unsymmetrical M−O bond length observed in these complexes; these differences in the magnitudes are reflected in the computed magnetic coupling.

As magnetic data could be well simulated with the model Hamiltonian $H = -2JS_1 \cdot S_2$, it is evident that Fe^{III} in **1** and **2** is in a high-spin state throughout the temperature range 2−290 K. DFT-computed spin state energies of a model $Fe^{III}Zn^{II}$ compound constructed on replacing Ni^{II} in **2A** by Zn^{II} and t_{2g}−e_g splitting of the Fe^{III} center in **2A** also clearly indicate that Fe^{III} is in a high-spin state and spin crossover is not possible (Figure S3, Supporting Information).

With this, we set out to develop magneto-structural correlations for a diphenoxo-bridged $Fe^{III}Ni^{II}$ dinuclear unit. Since the two μ-phenoxo bridges are the parts of the macrocyclic ligand system and one structural variation at a time demands variation of Fe⋯Ni and O⋯O distances, a model complex has been constructed for complex **1** (Figure S4 in the Supporting Information). The calculation of J for this model is different from that for the original complex, with the computed J being 1.6 cm^{-1}, but we believe that this model is good enough to understand the trend observed among different structural parameters.

J versus Bond Angle Correlation. The correlation on average Fe−O−Ni angle has been developed and is shown in Figure 9. The J values decrease with an increase in average Fe−O−Ni angle up to around 125°. This is due to predominant $d_{x^2-y^2}|p|d_{x^2-y^2}$ overlap. After 125°, a steep increase in J value is observed. At first instance, this result seems surprising, as we are observing ferromagnetic interactions at large Fe−O−Ni angles. However, such a trend has already been noted in di-μ-oxo Cu(II) complexes.[8c] At larger angles the Ni−O and Fe−O σ* orbitals gradually lose the major metal d contribution and, at extremely larger angles, a significant electron transfer from these σ* orbitals to the O−O π* orbital is taking place, indicating an O−O interaction. It is noted here that at the extreme angle of 133°, the
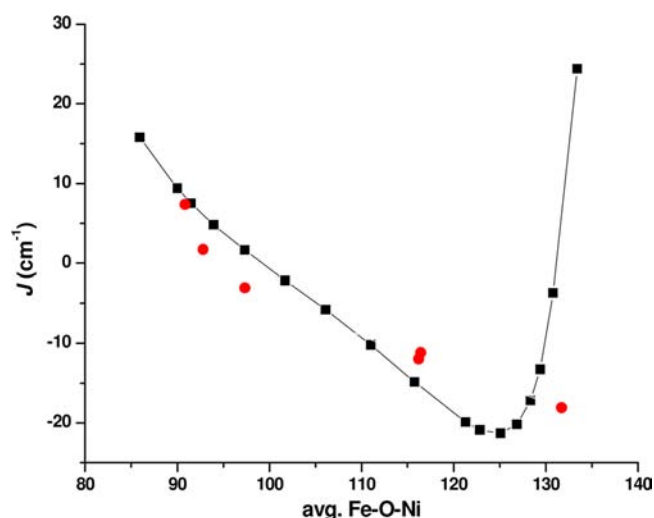
O⋯O distance is merely 1.60 Å, indicating a rather strong O⋯O interaction. This statement is verified by plotting the spin density of Fe^{III} together with the average spin density on the oxygen atoms, and this clearly indicates that the spin population on the oxygen atoms increases steeply at a larger Fe−O−Ni bond angle (Figure 10a). A steep decrease in Fe^{III} (also Ni^{II}) is accompanied by a steep increase in oxygen, indicating a strong oxygen−oxygen interaction and strong ferromagnetic coupling. The distortion for smaller and larger angles costs ca. 100 kJ/mol for structures up to 120° while much larger angles steeply raise the energy penalty; this is due to O⋯O interactions being the dominant factor (see Figure S5 in the Supporting Information). Among the correlations developed (see below), the Fe−O−Ni angle is the most important, as this parameter induces changes in J values of about 40 cm^{-1} while the changes in magnitude by other parameters are minimal.

J versus Bond Distance Correlation. The average Fe/Ni−O distance correlation developed is shown in Figure 10b (see also Figure S6 in the Supporting Information for experimental points). The J value steadily decreases with an increase in the average distance, tending toward less ferromagnetic J at greater distances. This is somewhat expected from the strong axial type d orbital overlap detected for this complex; as the distance increases the overlap decreases, leading to a smaller ferromagnetic J value at longer bond distances. This correlation, however, is expected to saturate at longer distance, and it is important to note here that the scale of change is much smaller as compared to the bond angle correlation.

J versus Fe−O−Ni−O Dihedral Angle Correlation. The third correlation, J versus Fe−O−Ni−O dihedral angle, is shown in Figure 10c (see also Figure S6 in the Supporting Information for experimental points). Initially, the J value decreases with a increase in the dihedral angle value and reaches saturation at higher angles. The spin densities on Fe^{III} and Ni^{II} along with different dihedral angles reveal that there is an antagonizing behavior where Fe^{III} spin density increases while Ni^{II} spin density decreases initially while at a higher angle the Fe^{III} spin density steeply decreases. This indicates that, at greater dihedral angles, a stronger delocalization is observed leading to an antiferromagnetic interaction at greater angles (see Table S2, Supporting Information).
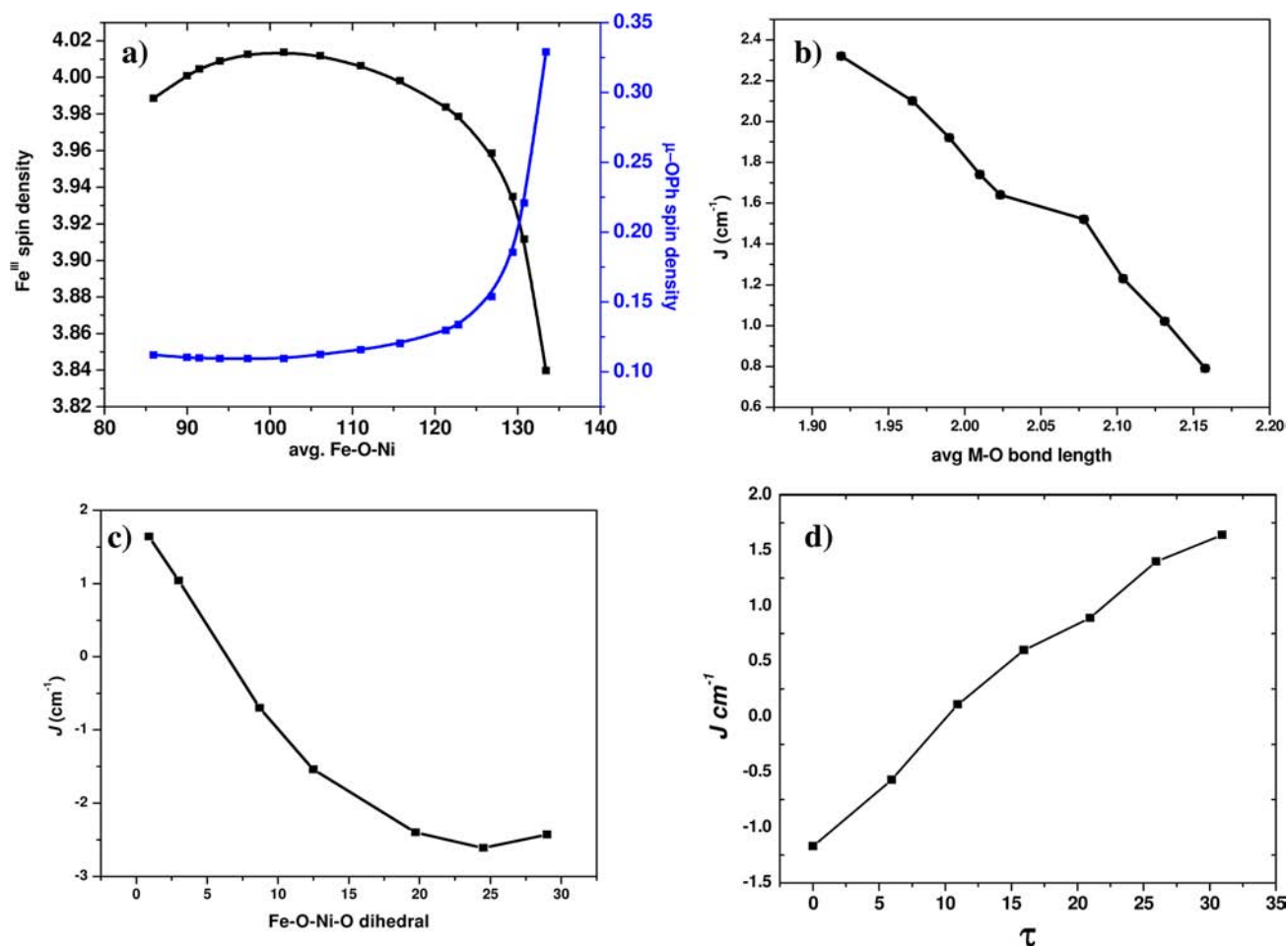
Figure 10. (a) Computed spin densities on the Fe^{III} and μ-phenoxo (average) atoms for various Fe−O−Ni angles. Magneto-structural correlations: (b) J versus average M−O (Fe−O and Ni−O distances); (c) J versus Fe−O−Ni−O dihedral angle; (d) J versus out-of-plane shift (τ) of the phenoxy group. The calculations for these correlations have been performed on the model complex **1A** (Figure S4, Supporting Information).

J versus Out-of-Plane Shift Correlation. The fourth correlation, J versus out-of-plane shift (τ) of the phenoxo group, has also been developed and is shown in Figure 10d (see also Figure S6 in the Supporting Information for experimental points). As we can see from this figure, an increase in the τ value increases the ferromagnetic J value and the molecule exhibits ferromagnetic exchange at higher τ value. The antiferromagnetic contribution to J decreases by increasing the τ parameter because the interaction between the oxygen and the phenyl group in plane orbitals (when τ is set to 0) weakens, leading to weaker overlap between the magnetic orbitals and stronger ferromagnetic exchange, as observed in Figure 10b.

■ CONCLUSIONS

The bis(μ-phenoxo) $Fe^{III}Ni^{II}$ compound $[Fe^{III}(N_3)_2LNi^{II}(H_2O)(CH_3CN)](ClO_4)$ (**1**) and the cocrystalline bis(μ-phenoxo)-μ-acetate/bis(μ-phenoxo)-bis(μ-acetate) $Fe^{III}Ni^{II}$ compound $\{[Fe^{III}(OAc)LNi^{II}(H_2O)(\mu\text{-OAc})]_{0.6}\cdot[Fe^{III}LNi^{II}(\mu\text{-OAc})_2]_{0.4}\}\cdot(ClO_4)\cdot1.1H_2O$ (**2**) are among the very rare examples of $Fe^{III}Ni^{II}$ compounds containing one or more phenoxo/hydroxo/alkoxo bridges. The antiferromagnetic interaction in **1** and ferromagnetic interaction in **2** reveal that our design to produce systems having remarkably different magnetic properties has been successful. Interestingly, the DFT calculated J values are nicely matched with the experimental J values of **1**, **2**, and previously reported μ-phenoxo-bis(μ-carboxylate) or μ-alkoxo-μ-diphenylphosphate

$Fe^{III}Ni^{II}$ compounds. Therefore, as no experimental J value is available for a μ-phenoxo-bis(μ-carboxylate) $Fe^{III}Ni^{II}$ system (**5**), the DFT calculated J value (-6.9 cm^{-1}) can be taken as the exchange coupling constant for this compound.

The countercomplementarity effect of carboxylate in heterobridged μ-phenoxo/hydroxo/alkoxo-μ-carboxylate dicopper(II) compounds can be easily understood from the orbital model, which is rather simple due to a single magnetic orbital per metal ion. This idea is usually extended to the heterobridged systems of other metal ions having more than one magnetic orbital. However, in the latter cases, the situation may be complicated due to several possible combinations of magnetic orbitals. Therefore, a clear demonstration of the countercomplementarity effect of an acetate moiety in $Fe^{III}Ni^{II}$ systems from DFT calculations in the present investigation deserves attention, although it has also been shown that the countercomplementarity effect is smaller and not additive. It has also been demonstrated that the countercomplementarity effect of carboxylate is operative via the d_{z^2} orbital. Again, the more prominent role of terminal bridging acetate in comparison to the bridging acetate is an interesting observation, which has been also clarified in terms of MO analyses. The DFT computed magneto-structural correlations of J with several parameters (Fe−O−Ni angle, average Fe/Ni−O distance, Fe−O−Ni−O dihedral angle, and out-of-plane shift of the phenoxo group) of the diphenoxo-bridged $Fe^{III}Ni^{II}$ systems, as determined here, are among the only few correlations

(theoretical or experimental) in heteronuclear systems and are the first in any type of $Fe^{III}Ni^{II}$ system. The profiles of magneto-structural correlations here have been justified also in terms of structural parameters or in terms of DFT-computed spin densities. The first examples of magneto-structural correlations, as demonstrated here, will be hopefully useful in analyzing the magnetic behavior of $Fe^{III}Ni^{II}$ polynuclear clusters in terms of pairwise interactions and therefore will also be useful in designing $Fe^{III}Ni^{II}$-based SMMs.

With regard to the countercomplementarity effect of carboxylate and the magneto-structural correlations established here, all of the factors are not in the same line to govern antiferromagnetic interactions in **1** and ferromagnetic interactions in **2**. However, the electronic origin of the interactions has been nicely understood from MO analysis.

■ ASSOCIATED CONTENT

Ⓢ Supporting Information

Text, figures, tables, and CIF files giving crystallographic data for **1** and **2**, a description of the supramolecular topology in **1** and **2**, Figures S1−S5, and Tables S1 and S2. This material is available free of charge via the Internet at http://pubs.acs.org.

■ AUTHOR INFORMATION

Corresponding Authors
*E-mail for G.R.: rajaraman@chem.iitb.ac.in.
*E-mail for S.M.: sm_cu_chem@yahoo.co.in.

Notes
The authors declare no competing financial interest.

■ ACKNOWLEDGMENTS

■ REFERENCES

(1) (a) Guha, B. *Proc. R. Soc. London* **1951**, *A206*, 353. (b) Bleaney, B.; Bowers, K. D. *Proc. R. Soc. London* **1952**, *A214*, 451.

(2) (a) Kahn, O. *Molecular Magnetism*; VCH: New York, 1993. (b) *Magneto-Structural Correlations in Exchange Coupled Systems*; Willet, R. D., Gatteschi, D., Kahn, O., Eds.; Reidel: Dordrecht, The Netherlands, 1985.

(3) (a) Crawford, V. M.; Richardson, H. W.; Wasson, J. R.; Hodgson, D. J.; Hatfield, W. E. *Inorg. Chem.* **1976**, *15*, 2107. (b) Merz, L.; Haase, W. *J. Chem. Soc., Dalton Trans.* **1980**, 875. (c) Thompson, L. K.; Mandal, S. K.; Tandon, S. S.; Bridson, J. N.; Park, M. K. *Inorg. Chem.* **1996**, *35*, 3117. (d) Wichmann, O.; Sopo, H.; Colacio, E.; Mota, A. J.; Sillanpää, R. *Eur. J. Inorg. Chem.* **2009**, 4877. (e) Laborda, S.; Clérac, R.; Anson, C. E.; Powell, A. K. *Inorg. Chem.* **2004**, *43*, 5931. (f) Botana, L.; Ruiz, J.; Seco, J. M.; Mota, A. J.; Rodríguez-Diéguez, A.; Sillanpää, R.; Colacio, E. *Dalton Trans.* **2011**, *40*, 12462. (g) Roundhill, S. G. N.; Roundhill, D. M.; Bloomquist, D. R.; Landee, C.; Willett, R. D.; Dooley, D. M.; Gray, H. B. *Inorg. Chem.* **1979**, *18*, 831.

(4) (a) Nanda, K. K.; Thompson, L. K.; Bridson, J. N.; Nag, K. *Chem. Commun.* **1994**, 1337. (b) Palacios, M. A.; Mota, A. J.; Perea-Buceta, J. E.; White, F. J.; Brechin, E. K.; Colacio, E. *Inorg. Chem.* **2010**, *49*, 10156. (c) Sasmal, S.; Hazra, S.; Kundu, P.; Dutta, S.; Rajaraman, G.; Sañudo, E. C.; Mohanta, S. *Inorg. Chem.* **2011**, *50*, 7257. (d) Sasmal, S.; Hazra, S.; Kundu, P.; Majumder, S.; Aliaga-Alcalde, N.; Ruiz, E.; Mohanta, S. *Inorg. Chem.* **2010**, *49*, 9517.

(5) (a) Kurtz, D. M., Jr. *Chem. Rev.* **1990**, *90*, 585. (b) Weihe, H.; Güdel, H. U. *J. Am. Chem. Soc.* **1997**, *119*, 6539. (c) Gall, F. L.; Biani, F. F. d.; Caneschi, A.; Cinelli, P.; Cornia, A.; Fabretti, A. C.; Gatteschi, D. *Inorg. Chim. Acta* **1997**, *262*, 123. (d) Hänninen, M. M.; Colacio, E.; Mota, A. J.; Sillanpää, R. *Eur. J. Inorg. Chem.* **2011**, 1990. (e) Werner, R.; Ostrovsky, S.; Griesar, K.; Haase, W. *Inorg. Chim. Acta* **2001**, *326*, 78. (f) Gorun, S. M.; Lippard, S. J. *Inorg. Chem.* **1991**, *30*, 1625. (g) Cañada-Vilalta, C.; O'Brien, T. A.; Brechin, E. K.; Pink, M.; Davidson, E. R.; Christou, G. *Inorg. Chem.* **2004**, *43*, 5505.

(6) (a) Law, N. A.; Kampf, J. W.; Pecoraro, V. L. *Inorg. Chim. Acta* **2000**, *297*, 252. (b) Berg, N.; Rajeshkumar, T.; Taylor, S. M.; Brechin, E. K.; Rajaraman, G.; Jones, L. F. *Chem. Eur. J.* **2012**, *18*, 5906. (c) Niemann, A.; Bossek, U.; Wieghardt, K.; Butzlaff, C.; Trautwein, A. X.; Nuber, B. *Angew. Chem., Int. Ed. Engl.* **1992**, *31*, 311.

(7) (a) Costes, J.-P.; Dahan, F.; Dupuis, A. *Inorg. Chem.* **2000**, *39*, 165. (b) Mohanta, S.; Nanda, K. K.; Thompson, L. K.; Flörke, U.; Nag, K. *Inorg. Chem.* **1998**, *37*, 1465.

(8) (a) Venegas-Yazigi, D.; Aravena, D.; Spodine, E.; Ruiz, E.; Alvarez, S. *Coord. Chem. Rev.* **2010**, *254*, 2086. (b) Charlot, M. F.; Kahn, O.; Jeannin, S.; Jeannin, Y. *Inorg. Chem.* **1980**, *19*, 1410. (c) Ruiz, E.; de Graaf, C.; Alemany, P.; Alvarez, S. *J. Phys. Chem. A* **2002**, *106*, 4938. (d) Ruiz, E.; Alemany, P.; Alvarez, S.; Cano, J. *J. Am. Chem. Soc.* **1997**, *119*, 1297. (e) Rodríguez-Fortea, A.; Alemany, P.; Alvarez, S.; Ruiz, E. *Inorg. Chem.* **2002**, *41*, 3769. (f) Ruiz, E.; Cano, J.; Alvarez, S.; Alemany, P. *J. Am. Chem. Soc.* **1998**, *120*, 11122. (g) Triki, S.; Gómez-García, C. J.; Ruiz, E.; Sala-Pala, J. *Inorg. Chem.* **2005**, *44*, 5501. (h) Biani, F. F. d.; Ruiz, E.; Cano, J.; Novoa, J. J.; Alvarez, S. *Inorg. Chem.* **2000**, *39*, 3221.

(9) Manca, G.; Cano, J.; Ruiz, E. *Inorg. Chem.* **2009**, *48*, 3139.

(10) (a) Rajaraman, G.; Totti, F.; Bencini, A.; Caneschi, A.; Sessoli, R.; Gatteschi, D. *Dalton Trans.* **2009**, 3153. (b) Singh, S. K.; Tibrewal, N. K.; Rajaraman, G. *Dalton Trans.* **2011**, *40*, 10897. (c) Rajeshkumar, T.; Rajaraman, G. *Chem. Commun.* **2012**, *48*, 7856.

(11) (a) Caneschi, A.; Gatteschi, D.; Sessoli, R.; Barra, A. L.; Brunel, L. C.; Guillot, M. *J. Am. Chem. Soc.* **1991**, *113*, 5873. (b) Sessoli, R.; Gatteschi, D.; Caneschi, A.; Novak, M. A. *Nature* **1993**, *365*, 141.

(12) (a) Aromí, G.; Brechin, E. K. *Struct. Bonding (Berlin)* **2006**, *122*, 1. (b) Murrie, M. *Chem. Soc. Rev.* **2010**, *39*, 1986. (c) Stamatatos, T. C.; Christou, G. *Inorg. Chem.* **2009**, *48*, 3308. (d) Mukherjee, S.; Abboud, K. A.; Wernsdorfer, W.; Christou, G. *Inorg. Chem.* **2013**, *52*, 873.

(13) (a) Woodruff, D. N.; Winpenny, R. E. P.; Layfield, R. A. *Chem. Rev.* **2013**, *113*, 5110. (b) Rinehart, J. D.; Long, J. R. *Chem. Sci.* **2011**, *2*, 2078. (c) Sorace, L.; Benelli, C.; Gatteschi, D. *Chem. Soc. Rev.* **2011**, *40*, 3092. (d) Guo, Y.-N.; Xu, G.-F.; Guo, Y.; Tang, J. *Dalton Trans.* **2011**, *40*, 9953. (e) Sessoli, R.; Powell, A. K. *Coord. Chem. Rev.* **2009**, *253*, 2328.

(14) (a) Tasiopoulos, A. J.; Vinslava, A.; Wernsdorfer, W.; Abboud, K. A.; Christou, G. *Angew. Chem., Int. Ed.* **2004**, *43*, 2117. (b) Milios, C. J.; Vinslava, A.; Wernsdorfer, W.; Moggach, S.; Parsons, S.; Perlepes, S. P.; Christou, G.; Brechin, E. K. *J. Am. Chem. Soc.* **2007**, *129*, 2754. (c) Habib, F.; Brunet, G.; Loiseau, F.; Pathmalingam, T.; Burchell, T. J.; Beauchemin, A. M.; Wernsdorfer, W.; Clérac, R.; Murugesu, M. *Inorg. Chem.* **2013**, *52*, 1296. (d) Ako, A. M.; Mereacre, V.; Lan, Y.; Wernsdorfer, W.; Clérac, R.; Anson, C. E.; Powell, A. K. *Inorg. Chem.* **2010**, *49*, 1. (e) Hazra, S.; Sasmal, S.; Fleck, M.; Grandjean, F.; Sougrati, M. T.; Ghosh, M.; Harris, T. D.; Bonville, P.; Long, G. J.; Mohanta, S. *J. Chem. Phys.* **2011**, *134*, 174507.

(15) (a) Ishikawa, N.; Sugita, M.; Ishikawa, T.; Koshihara, S.-y.; Kaizu, Y. *J. Am. Chem. Soc.* **2003**, *125*, 8694. (b) Gonidec, M.; Biagi, R.; Corradini, V.; Moro, F.; Renzi, V. D.; Pennino, U. d.; Summa, D.; Muccioli, L.; Zannoni, C.; Amabilino, D. B.; Veciana, J. *J. Am. Chem. Soc.* **2011**, *133*, 6603. (c) Rinehart, J. D.; Fang, M.; Evans, W. J.; Long, J. R. *Nat. Chem.* **2011**, *3*, 538. (d) Guo, Y.-N.; Xu, G.-F.; Wernsdorfer, W.; Ungur, L.; Guo, Y.; Tang, J.; Zhang, H.-J.; Chibotaru, L. F.; Powell, A. K. *J. Am. Chem. Soc.* **2011**, *133*, 11948. (e) Tuna, F.; Smith, C. A.; Bodensteiner, M.; Ungur, L.; Chibotaru, L. F.; McInnes, E. J. L.; Winpenny, R. E. P.; Collison, D.; Layfield, R. A. *Angew. Chem., Int. Ed.*

2012, *51*, 6976. (f) Anwar, M. U.; Tandon, S. S.; Dawe, L. N.; Habib, F.; Murugesu, M.; Thompson, L. K. *Inorg. Chem.* **2012**, *51*, 1028.

(16) (a) Colacio, E.; Ruiz-Sanchez, J.; White, F. J.; Brechin, E. K. *Inorg. Chem.* **2011**, *50*, 7268. (b) Karotsis, G.; Kennedy, S.; Teat, S. J.; Beavers, C. M.; Fowler, D. A.; Morales, J. J.; Evangelisti, M.; Dalgarno, S. J.; Brechin, E. K. *J. Am. Chem. Soc.* **2010**, *132*, 12983. (c) Feltham, H. L. C.; Clérac, R.; Ungur, L.; Chibotaru, L. F.; Powell, A. K.; Brooker, S. *Inorg. Chem.* **2013**, *52*, 3236. (d) Mereacre, V.; Lan, Y.; Clérac, R.; Ako, A. M.; Wernsdorfer, W.; Buth, G.; Anson, C. E.; Powell, A. K. *Inorg. Chem.* **2011**, *50*, 12001. (e) Abbas, G.; Lan, Y.; Mereacre, V.; Wernsdorfer, W.; Clérac, R.; Buth, G.; Sougrati, M. T.; Grandjean, F.; Long, G. J.; Anson, C. E.; Powell, A. K. *Inorg. Chem.* **2009**, *48*, 9345.

(17) (a) Loth, S.; Baumann, S.; Lutz, C. P.; Eigler, D. M.; Heinrich, A. J. *Science* **2012**, *335*, 196. (b) Mannini, M.; Pineider, F.; Sainctavit, P.; Danieli, C.; Otero, E.; Sciancalepore, C.; Talarico, A. M.; Arrio, M.-A.; Cornia, A.; Gatteschi, D.; Sessoli, R. *Nat. Mater.* **2009**, *8*, 194.

(18) (a) Cremades, E.; Gómez-Coca, S.; Aravena, D.; Alvarez, S.; Ruiz, E. *J. Am. Chem. Soc.* **2012**, *134*, 10532. (b) Toma, L. M.; Ruiz-Pérez, C.; Lloret, F.; Julve, M. *Inorg. Chem.* **2012**, *51*, 1216. (c) Ruiz, E.; Cano, J.; Alvarez, S.; Caneschi, A.; Gatteschi, D. *J. Am. Chem. Soc.* **2003**, *125*, 6791. (d) Rajaraman, G.; Cano, J.; Brechin, E. K.; McInnes, E. J. L. *Chem. Commun.* **2004**, 1476. (e) Christian, P.; Rajaraman, G.; Harrison, A.; Helliwell, M.; McDouall, J. J. W.; Raftery, J.; Winpenny, R. E. P. *Dalton Trans.* **2004**, 2550. (f) Rajaraman, G.; Murugesu, M.; Sañudo, E. C.; Soler, M.; Wernsdorfer, W.; Helliwell, M.; Muryn, C.; Raftery, J.; Teat, S. J.; Christou, G.; Brechin, E. K. *J. Am. Chem. Soc.* **2004**, *126*, 15445. (g) Hegetschweiler, K.; Morgenstern, B.; Zubieta, J.; Hagrman, P. J.; Lima, N.; Sessoli, R.; Totti, F. *Angew. Chem., Int. Ed.* **2004**, *43*, 3436.

(19) (a) Dutta, S. K.; Werner, R.; Flörke, U.; Mohanta, S.; Nanda, K. K.; Haase, W.; Nag, K. *Inorg. Chem.* **1996**, *35*, 2292. (b) Holman, T. R.; Juarez-Garcia, C.; Hendrich, M. P.; Que, L., Jr.; Münck, E. *J. Am. Chem. Soc.* **1990**, *112*, 7611. (c) Jarenmark, M.; Haukka, M.; Demeshko, S.; Tuczek, F.; Zuppiroli, L.; Meyer, F.; Nordlander, E. *Inorg. Chem.* **2011**, *50*, 3866. (d) Yin, L.-h.; Cheng, P.; Yan, S.-P.; Fu, X.-Q.; Li, J.; Liao, D.-Z.; Jiang, Z.-H. *Dalton Trans.* **2001**, 1398.

(20) (a) Volbeda, A.; Garcin, E.; Piras, C.; de Lacey, A. L.; Fernandez, V. M.; Hatchikian, E. C.; Frey, M.; Fontecilla-Camps, J. C. *J. Am. Chem. Soc.* **1996**, *118*, 12989. (b) Volbeda, A.; Charon, M.-H.; Piras, C.; Hatchikian, E. C.; Frey, M.; Fontecilla-Camps, J. C. *Nature* **1995**, *373*, 580.

(21) Olguín, J.; Brooker, S. *New J. Chem.* **2011**, *35*, 1242.

(22) Pilkington, N. H.; Robson, R. *Aust. J. Chem.* **1970**, *23*, 2225.

(23) Noodleman, L. *J. Chem. Phys.* **1981**, *74*, 5737.

(24) (a) Becke, A. D. *J. Chem. Phys.* **1993**, *98*, 5648. (b) Schäfer, A.; Horn, H.; Ahlrichs, R. *J. Chem. Phys.* **1992**, *97*, 2571. (c) Schäfer, A.; Huber, C.; Ahlrichs, R. *J. Chem. Phys.* **1994**, *100*, 5829.

(25) Frisch, M. J.; et al. *Gaussian 09*; Gaussian, Inc., Pittsburgh, PA, 2009.

(26) (a) *APEX-II, SAINT-Plus, and TWINABS*; Bruker-Nonius AXS Inc.: Madison, WI, USA, 2004. (b) Sheldrick, G. M. *SAINT (version 6.02) and SADABS (version 2.03)*; Bruker AXS lnc., Madison, WI, USA, 2002. (c) *SHELXTL (version 6.10)*; Bruker AXS Inc., Madison, WI, USA, 2002. (d) Sheldrick, G. M. *SHELXL-97, Crystal Structure Refinement Program*; University of Göttingen, Göttingen, Germany, 1997.

(27) Bill, E. *julX Program*; Max-Planck-Institut für Bioanorganische Chemie, Mülheim an der Ruhr, Germany, 2008.

(28) Batista, S. C.; Neves, A.; Bortoluzzi, A. J.; Vencato, I.; Peralta, R. A.; Szpoganicz, B.; Aires, V. V. E.; Terenzi, H.; Severino, P. C. *Inorg. Chem. Commun.* **2003**, *6*, 1161.

(29) The Cambridge Structural Database (CSD), Version 5.34, 2012.

(30) Desplanches, C.; Ruiz, E.; Rodrigues-Fortea, A.; Alvarez, S. *J. Am. Chem. Soc.* **2002**, *124*, 5197.

(31) Mereacre, V.; Baniodeh, A.; Anson, C. E.; Powell, A. K. *J. Am. Chem. Soc.* **2011**, *133*, 15335.